

Signatures of a gearwheel quantum spin liquid in a spin- $\frac{1}{2}$ pyrochlore molybdate Heisenberg antiferromagnet

Yasir Iqbal,^{1,*} Tobias Müller,² Kira Riedl,³ Johannes Reuther,^{4,5} Stephan Rachel,^{6,7} Roser Valentí,³ Michel J. P. Gingras,^{8,9,10} Ronny Thomale,² and Harald O. Jeschke¹¹

¹*Department of Physics, Indian Institute of Technology Madras, Chennai, 600036, India*

²*Institute for Theoretical Physics and Astrophysics, Julius-Maximilian's University of Würzburg, Am Hubland, D-97074 Würzburg, Germany*

³*Institut für Theoretische Physik, Goethe-Universität Frankfurt, Max-von-Laue-Straße 1, D-60438 Frankfurt am Main, Germany*

⁴*Dahlem Center for Complex Quantum Systems and Fachbereich Physik, Freie Universität Berlin, D-14195 Berlin, Germany*

⁵*Helmholtz-Zentrum Berlin für Materialien und Energie, D-14109 Berlin, Germany*

⁶*School of Physics, The University of Melbourne, Parkville, VIC 3010, Australia*

⁷*Institut für Theoretische Physik, Technische Universität Dresden, D-01062 Dresden, Germany*

⁸*Perimeter Institute for Theoretical Physics, Waterloo, Ontario, Canada N2L 5G7*

⁹*Department of Physics and Astronomy, University of Waterloo, Waterloo, Ontario, Canada N2L 3G1*

¹⁰*Canadian Institute for Advanced Research, 180 Dundas Street West, Toronto, Ontario, Canada M5G 1Z8*

¹¹*Research Institute for Interdisciplinary Science, Okayama University, 3-1-1 Tsushima-naka, Kita-ku, Okayama 700-8530, Japan*

(Received 24 May 2017; revised manuscript received 5 October 2017; published 13 December 2017)

We theoretically investigate the low-temperature phase of the recently synthesized $\text{Lu}_2\text{Mo}_2\text{O}_5\text{N}_2$ material, an extraordinarily rare realization of a $S = 1/2$ three-dimensional pyrochlore Heisenberg antiferromagnet in which Mo^{5+} are the $S = 1/2$ magnetic species. Despite a Curie-Weiss temperature (Θ_{CW}) of $-121(1)$ K, experiments have found no signature of magnetic ordering or spin freezing down to $T^* \approx 0.5$ K. Using density functional theory, we find that the compound is well described by a Heisenberg model with exchange parameters up to third nearest neighbors. The analysis of this model via the pseudofermion functional renormalization group method reveals paramagnetic behavior down to a temperature of at least $T = |\Theta_{\text{CW}}|/100$, in agreement with the experimental findings hinting at a possible three-dimensional quantum spin liquid. The spin susceptibility profile in reciprocal space shows momentum-dependent features forming a “gearwheel” pattern, characterizing what may be viewed as a molten version of a chiral noncoplanar incommensurate spiral order under the action of quantum fluctuations. Our calculated reciprocal space susceptibility maps provide benchmarks for future neutron scattering experiments on single crystals of $\text{Lu}_2\text{Mo}_2\text{O}_5\text{N}_2$.

DOI: 10.1103/PhysRevMaterials.1.071201

Introduction. A quantum spin liquid (QSL) is an exotic strongly correlated paramagnetic quantum state of matter [1–3] that lacks conventional long-range magnetic order down to absolute zero temperature and is characterized by nontrivial spin entanglement and low-energy fractionalized spin excitations [4–6]. One of the ideal settings to explore QSL physics is provided by systems in which the magnetic moments reside on either a two- or three-dimensional network of corner-shared (CS) triangles or tetrahedra and interact with an isotropic nearest-neighbor antiferromagnetic Heisenberg exchange Hamiltonian. The promise of such systems stems, in part, from their low propensity to order even at the classical level [7–9]. Materials with magnetic species described by an (effective) $S = 1/2$ operator are expected to display the most extreme quantum behaviors, as suggested by numerous theoretical and numerical works spanning over 25 years [10–18], and are manifestly of significant interest.

While one might legitimately expect that single-ion anisotropy and exchange anisotropy would much undermine the likeliness of a QSL, the proposals that QSL states may be realized in systems described by effective $S = 1/2$ degrees of freedom, but with strongly anisotropic bilinear spin-spin couplings originating from large spin-orbit interactions, are exciting developments in the field. These include “Kitaev”

materials [19–24] based on Ir^{4+} or Ru^{3+} , and “quantum spin ice” (QSI) [25–28] pyrochlore oxide materials with trivalent rare-earth ions.

In the above Heisenberg antiferromagnets, Kitaev and QSI systems, one has at hand a reference (idealized) Hamiltonian \mathcal{H}_0 as the model presumed to host a QSL state. The general mindset in the field has been to consider materials whose true Hamiltonian, $\mathcal{H} = \mathcal{H}_0 + \mathcal{H}'$, may not be “too far” from \mathcal{H}_0 in terms of all material-relevant perturbations \mathcal{H}' . From a material perspective, the search and discovery of QSL phases thus require some luck so that \mathcal{H}' is sufficiently weak that long-range order is evaded. The experimental investigation of such potential QSL materials requires the synthesis of single crystals which, albeit being at times a daunting challenge, is a necessary one as it allows to expose the nontrivial momentum dispersion of low-energy excitations characterizing QSL states [29–31].

A prime candidate for a QSL phase in two dimensions is the herbertsmithite kagome material where long-range exchange beyond nearest neighbor as well as the Dzyaloshinsky-Moriya (DM) interaction might be subcritical to drive this compound to a magnetic long-range ordered state [29,32,33]. Illustrating further the subcritical role of further interactions, one may note the kapellasite kagome compound [34,35], which is altogether described at “zeroth order” by a complex spin Hamiltonian with numerous competing interactions beyond nearest neighbor, landing it in a parameter space island where a QSL may be realized [36–38]. Nevertheless, the

*yiqbal@physics.iitm.ac.in

number of candidates for QSL behavior in two dimensions is small and the situation for three-dimensional materials is even more disconcerting. The pyrochlore lattice of CS tetrahedra, occurring in pyrochlore oxides and spinel magnetic materials, is an attractive architecture to search for QSLs [10–13,39–43]. Unfortunately, most materials in these two families either develop long-range magnetic order or display a spin-glass-like freezing at low temperature, hence averting a QSL state. Similarly, $\text{Na}_4\text{Ir}_3\text{O}_8$ [44], an antiferromagnetic spin- $\frac{1}{2}$ material with a three-dimensional hyperkagome lattice of CS triangles, also exhibits a spin freezing below about 7 K [45]. The MgTi_2O_4 spinel has $S = 1/2$ Ti^{3+} moments, but structurally distorts at low temperature [46]. Finally, most Kitaev materials so far identified display long-range order and the behaviors of the best QSI candidates remain far from being well rationalized [23].

One may thus offer an executive summary of the experimental situation, especially for three-dimensional materials: In all cases, the perturbations \mathcal{H}' are above a critical value and preempt the formation of a QSL. At this juncture, a convergence of opportunities, from the point of view of (i) potential QSL material candidates and (ii) an ability to model its \mathcal{H} and expose its QSL nature with state-of-the-art numerical methods, is required to encourage the significant efforts in the synthesis of pertinent single crystals of three-dimensional QSL candidates. In this context, we propose in this Rapid Communication that $\text{Lu}_2\text{Mo}_2\text{O}_5\text{N}_2$ is a candidate much deserving such effort and subsequent investigation.

$\text{Lu}_2\text{Mo}_2\text{O}_5\text{N}_2$ is a pyrochlore Heisenberg antiferromagnet with Mo^{5+} $S = 1/2$ moments that fail to develop long-range order or spin freezing down to $T^* \approx 0.5$ K, despite a Curie-Weiss temperature of $\Theta_{\text{CW}} = -121(1)$ K [47]. Notwithstanding the appeal of its $S = 1/2$ \mathcal{H}_0 Heisenberg antiferromagnetic nature, we characterize in this work the leading perturbation \mathcal{H}' of $\text{Lu}_2\text{Mo}_2\text{O}_5\text{N}_2$ in the hope of identifying a material with an innocuous \mathcal{H}' such that it does not induce long-range magnetic order.

While the nonmagnetic random site O/N disorder might certainly be worth considering at a later stage, in this Rapid Communication, as a first step in fleshing out the leading physics at play in $\text{Lu}_2\text{Mo}_2\text{O}_5\text{N}_2$, we model this material as an effective homogeneous $S = 1/2$ pyrochlore magnet. We apply a combination of (i) density functional theory (DFT) determination of the Hamiltonian parameters where the random O/N occupation is modeled using the virtual crystal approximation [48], (ii) a $S = 1/2$ pseudofermion functional renormalization group (PFFRG) study of the resulting Heisenberg Hamiltonian, and (iii) an analysis of the multiple- \mathbf{k} spiral order that is realized for a classical version of the spin model derived from DFT. We establish the nature of the perturbation \mathcal{H}' and find it to be *meek* at inducing long-range order—likely the one key factor for the failure of this material to freeze or order down to $|T^*/\Theta_{\text{CW}}| \ll 1$. It is shown that the long-range (third-nearest-neighbor) exchange coupling, in particular, J_{3a} [see Fig. 1 and Eq. (1)], is crucial for defining a minimal material-relevant model Hamiltonian for $\text{Lu}_2\text{Mo}_2\text{O}_5\text{N}_2$, as found for chromium spinels [49,50]. For the model of Eq. (1) below, the PFFRG shows an absence of magnetic order down to temperatures $T^* \cong |\Theta_{\text{CW}}|/100$, in agreement with experiment. A classical analysis [51–55] of this model identifies

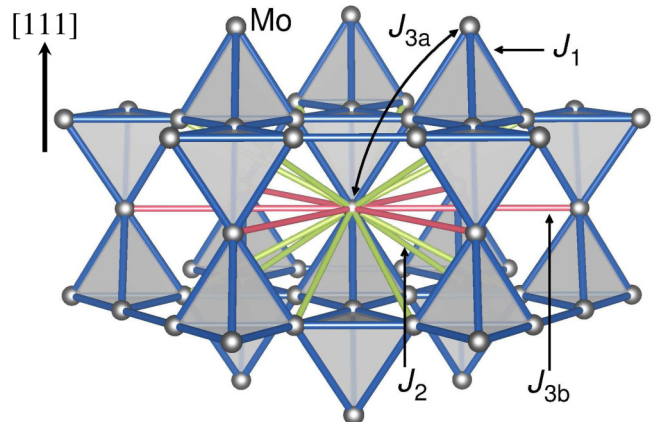


FIG. 1. Leading exchange paths in the pyrochlore lattice of $\text{Lu}_2\text{Mo}_2\text{O}_5\text{N}_2$. Only the Mo^{5+} ions are shown.

a noncoplanar triple- \mathbf{k} incommensurate spiral order as the parent classical state, whose melting by quantum fluctuations, would give a suitable phenomenological frame to describe the observed quantum spin liquid, possibly of chiral nature, and its \mathbf{k} -dependent spin susceptibility fingerprint.

Results. The minimal model for $\text{Lu}_2\text{Mo}_2\text{O}_5\text{N}_2$ extracted from our DFT calculations [37,57] is given by a four-parameter isotropic $S = 1/2$ Heisenberg model,

$$\hat{\mathcal{H}} = J_1 \sum_{\langle i,j \rangle_1} \hat{\mathbf{S}}_i \cdot \hat{\mathbf{S}}_j + J_2 \sum_{\langle i,j \rangle_2} \hat{\mathbf{S}}_i \cdot \hat{\mathbf{S}}_j + J_{3a} \sum_{\langle i,j \rangle_{3a}} \hat{\mathbf{S}}_i \cdot \hat{\mathbf{S}}_j + J_{3b} \sum_{\langle i,j \rangle_{3b}} \hat{\mathbf{S}}_i \cdot \hat{\mathbf{S}}_j, \quad (1)$$

where $\hat{\mathbf{S}}_i$ is a quantum spin- $\frac{1}{2}$ operator at pyrochlore lattice site i . The indices $\langle i,j \rangle_{1(2)}$ denote sums over nearest-neighbor (second-nearest-neighbor) pairs of sites. There are two inequivalent third-nearest-neighbor sites, the $\langle i,j \rangle_{3a}$ (connecting two Mo^{5+} sites with a nearest-neighbor Mo^{5+} ion in between) and $\langle i,j \rangle_{3b}$ (across an empty hexagon in one of the three interpenetrating kagome lattices of the pyrochlore structure) (see Fig. 1). We find that $J_1, J_2, J_{3a} > 0$ are antiferromagnetic while $J_{3b} < 0$ is ferromagnetic (see Fig. 1). The set of exchange couplings corresponding to $U = 2.5$ eV (see Table S1 [56] and Fig. 2) give an estimate of the Curie-Weiss temperature $\Theta_{\text{CW}} = -125(4)$ K corresponding to the experimentally determined value of $\Theta_{\text{CW}} = -121(1)$ K. The couplings are found to be $(J_2, J_{3a}, J_{3b}) = (0.008, 0.23, -0.078)$ in units of J_1 , with $J_1 = 1$.

The PFFRG [20,58–65] calculations (see Ref. [56]) for the model Hamiltonian [Eq. (1)] for $\text{Lu}_2\text{Mo}_2\text{O}_5\text{N}_2$ were performed on a cluster of 2315 correlated sites with the longest spin-spin correlator being ~ 11.5 nearest-neighbor lattice spacings, which ensures an adequate \mathbf{k} -space resolution. The \mathbf{k} -space resolved spin susceptibility profile evaluated at the lowest temperature ($T = |\Theta_{\text{CW}}|/100 = 1.21$ K) is shown in Fig. 3(a). At a temperature which is two orders of magnitude smaller compared to Θ_{CW} , the diffused spectral weight along the edges of the Brillouin zone (with a slight enhancement at the W points) reflects the high degree of frustration in $\text{Lu}_2\text{Mo}_2\text{O}_5\text{N}_2$. Interestingly, analogous features

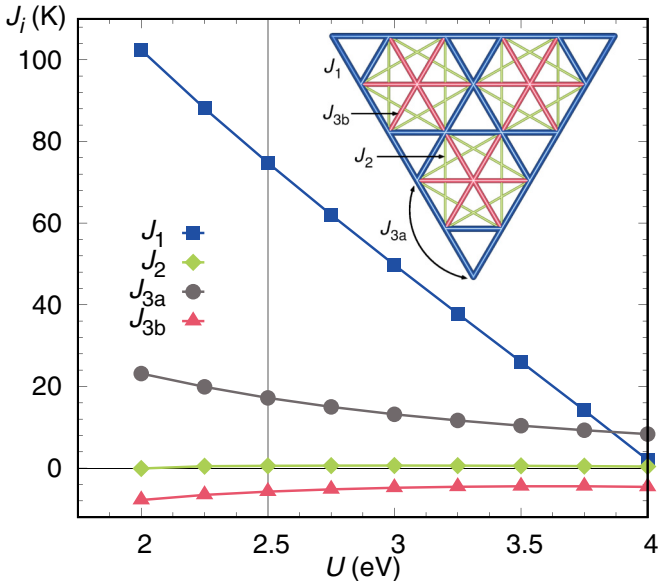


FIG. 2. Calculated exchange couplings for $\text{Lu}_2\text{Mo}_2\text{O}_5\text{N}_2$ as given in Table S1 [56]. Positive (negative) values correspond to antiferromagnetic (ferromagnetic) couplings. A generalized gradient approximation (GGA+U) functional with $J_H = 0.6$ eV was used. A vertical line marks the set of couplings which corresponds to a Curie-Weiss temperature of $\Theta_{\text{CW}} = -125(4)$ K, in good agreement with the experimental value of $-121(1)$ K. The inset shows a detail of the magnetic lattice with the first four exchange paths between Mo^{5+} ions, as viewed from the [111] direction (see Fig. 1).

in the spectral weight distribution around the boundary are also shared by the highly frustrated spin- $\frac{1}{2}$ kagome Heisenberg antiferromagnet [15,66,67]. Away from the boundaries, one observes soft maxima [marked by an arrow in Fig. 3(a)] at an incommensurate wave vector $\mathbf{k}_{\text{QSL}} = 2\pi(1.296, 1.296, 0)$ (and symmetry-related points). The \mathbf{k} -dependent features of the susceptibility are best visualized in the $[hh\ell]$ plane, i.e., $k_x = k_y$ plane [Fig. 3(b)]. Therein, we observe that the spectral weight at the pinch points $[(h,h,\ell) = (0,0,4\pi)]$ in Fig. 3(b)] is both substantially suppressed and smeared and, instead, redistributes to form hexagonal clusters [68], similar to what is observed in ZnCr_2O_4 [69]. This behavior is a consequence of the nonzero third-nearest-neighbor couplings J_{3a} and J_{3b} in Eq. (1), as has been argued in Ref. [53] on the basis of a classical analysis. In the $[hk0]$ plane, i.e., $k_z = 0$ plane [Fig. 3(c)], the characteristic spin susceptibility profile resembles a pattern of “gearwheels” and, following Ref. [70], we dub the spin liquid accordingly. The RG flow of the susceptibility tracked at the dominant wave vector \mathbf{k}_{QSL} is shown in Fig. 3(d) [71], wherein the observed oscillations at small temperature arise due to frequency discretization. Its monotonic increase as $T \rightarrow 0$ without any indication of a divergence points to the absence of a magnetic phase transition, in agreement with experiment [47]. We reach similar conclusions for exchange couplings corresponding to different values of U in the range 2 eV $\leqslant U \leqslant 3.25$ eV given in Table S1 [56].

In order to identify the classical long-range magnetic order associated with Eq. (1), we use both the PFFRG method, and an iterative energy minimization of the classical Hamiltonian [55]. In the $S \rightarrow \infty$ limit, the PFFRG flow equations permit

an exact analytic solution in the thermodynamic limit and the approach is equivalent to the Luttinger-Tisza method [65]. The resulting ground states on non-Bravais lattices are approximate, since only the global constraint $\sum_i |\mathbf{S}_i^2| = S^2 N$, where N is the total number of lattice sites, is enforced [72,73]. We find that under the RG flow, the two-particle vertex for the magnetic ordering (MO) wave vector, $\mathbf{k}_{\text{MO}} = 2\pi(1.305, 1.305, 0)$ [marked by an arrow in Fig. 3(e)] (and symmetry-related points), diverges at a Néel temperature of $T_N/J_1 \approx 0.625$, denoting the onset of an incommensurate magnetic order. The susceptibility profile evaluated at this ordering temperature is shown in Fig. 3(e). One observes that the susceptibility profile of the $S = 1/2$ model [Fig. 3(a)] may be viewed as a diffuse version of the one for the classical model [Fig. 3(e)]. Under the action of quantum fluctuations, the subdominant Bragg peaks on the hexagonal faces in Fig. 3(e) become diffuse to form a uniform ring in Fig. 3(a), while the dominant Bragg peaks at \mathbf{k}_{MO} smear out to form a gearwheel pattern, albeit leaving behind fingerprints [marked by an arrow in Fig. 3(a)]. The whitish “teeth” of the gearwheels seen in Fig. 3(c) can, likewise, be accounted for.

To obtain the exact classical ground state and, in addition, allow for possible lattice symmetry breaking, we perform an iterative classical energy minimization enforcing the constraint $|\mathbf{S}_i|^2 = S^2$ at each site i [73]. This yields a magnetic state that is a noncoplanar triple- \mathbf{k} structure composed of a superposition of three different spirals, each governed by an incommensurate wave vector \mathbf{k} . Moreover, we find that although the total spin per tetrahedron is not zero, the deviation is not energetically significant, being only a few percent of J_1 . This implies an approximate equivalence between the antiferromagnetic J_{3a} and ferromagnetic J_2 couplings [55,74], and accounts for the similarities of the orders found here with those of the J_1 - J_2 Heisenberg model [51,52,54]. The corresponding susceptibility profile is shown in Fig. 3(f), with the dominant Bragg peaks located at $\mathbf{k}'_{\text{MO}} = 2\pi(1.312, 1.312, 0)$ (in good agreement with \mathbf{k}_{MO}) (and symmetry-related points). The finite-size effects due to periodic boundary conditions cause Bragg peak splitting, and the results in Figs. 3(f) and 3(g) are shown after performing a Gaussian smoothing over the split peaks. It is important to note that the height of the Bragg peaks in the k_x - k_y and k_x - k_z planes are slightly different, but are roughly twice the height of the peak in the k_y - k_z plane [see Fig. 3(g)]. One may wonder whether the breaking of the cubic symmetry in the classical order could carry over to the $S = 1/2$ case and give rise to a nematic QSL [75,76].

Interestingly, the spin configuration of our classical magnetic order is chiral, namely, that the effect of a time-reversal operation $\mathbf{S} \rightarrow -\mathbf{S}$ cannot be undone by a global SO(3) spin rotation. This is precisely the defining characteristic of a *chiral* spin state [77] which, accordingly, exhibits a nonvanishing scalar spin chirality $\sim \mathbf{S}_i \cdot (\mathbf{S}_j \times \mathbf{S}_k)$. Indeed, we find that on every tetrahedron, any set of three spins gives a nonzero scalar spin chirality. The prospect of this chiral symmetry breaking carrying over to the QSL phase in the $S = 1/2$ model [78–80] sets the stage for a first realization in an insulator of a chiral spin liquid in three dimensions (see Refs. [81,82] for a metallic context). While we are unable to address this issue within the current implementation of PFFRG [56], an alternative route might be to proceed through a projective symmetry group

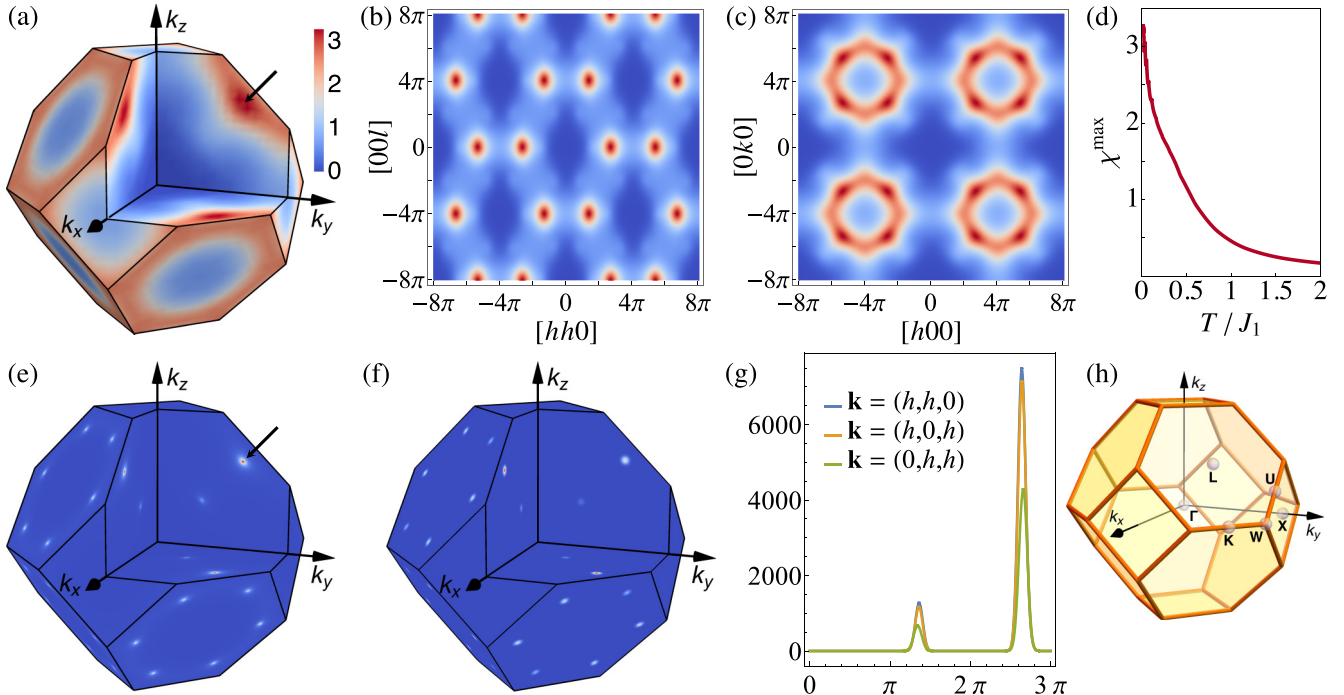


FIG. 3. First row: $S = 1/2$ PFFRG simulation of the model Hamiltonian [Eq. (1)] for $\text{Lu}_2\text{Mo}_2\text{O}_5\text{N}_2$. The magnetic susceptibility (in units of $1/J_1$) is shown at $T = |\Theta_{\text{CW}}|/100$ in the (a) full Brillouin zone, (b) $[hhl]$ plane, and (c) $[hk0]$ plane. (d) The RG flow of the dominant susceptibility. Second row: (e)–(g) Susceptibility profiles of the corresponding classical spin model obtained from (e) $S \rightarrow \infty$ limit of PFFRG, (f) iterative energy minimization, also shown along (g) selected cuts. (h) Brillouin zone of the pyrochlore lattice, a truncated octahedron, illustrating the high-symmetry points.

classification of chiral spin liquids along with a variational Monte Carlo analysis [83,84].

While our DFT calculations show that $\text{Lu}_2\text{Mo}_2\text{O}_5\text{N}_2$ is well approximated by a Heisenberg Hamiltonian, it merely serves as an effective minimal model. Indeed, a DM interaction term $\sim \mathbf{D}_{ij} \cdot (\hat{\mathbf{S}}_i \times \hat{\mathbf{S}}_j)$ [85] is also symmetry allowed. The Moriya rules [86] constrain this interaction to be one of two types, called “direct” or “indirect” [87,88]. Our DFT calculations of the DM term [89] find it to be “indirect” and estimate its magnitude to be $\approx 0.08 - 0.1 J_1$ (for a certain range of U values). Within PFFRG, a treatment of the DM interaction for the pyrochlore lattice would be computationally expensive [64]. However, a classical optimization calculation at $T = 0$ shows that a 8%–10% DM interaction does not significantly alter the nature of the classical state of the pure Heisenberg model (1). Indeed, we are unable to detect any shift in the Bragg peak positions within the available \mathbf{k} -space resolution, while only a minor redistribution of the spectral weight is observed.

Conclusion. We have shown that $\text{Lu}_2\text{Mo}_2\text{O}_5\text{N}_2$ is well described by an “extended” Heisenberg model. Our PFFRG analysis shows that the system remains paramagnetic down to a temperature that is at least two orders of magnitude smaller compared to the Curie-Weiss temperature Θ_{CW} . The spin susceptibility profile displays momentum-dependent features forming a pattern of gearwheels. These signatures lend support to the view that the supposed quantum spin liquid could be viewed as a molten version of a parent classical magnetic order, which is found to be a noncoplanar incommensurate

spiral. Our work provides a theoretical prediction for the characteristic spin susceptibility profile which should ultimately be compared with future neutron scattering experiments on single crystals. We hope that our work motivates further experimental investigations of the potentially very interesting $\text{Lu}_2\text{Mo}_2\text{O}_5\text{N}_2$ which may prove to be the first realization of a quantum spin liquid based on a spin- $\frac{1}{2}$ pyrochlore Heisenberg antiferromagnet, as our work here suggests by building on the report of Ref. [47].

Acknowledgments. We thank F. Becca, S. Bieri, L. Clark, I. I. Mazin, and J. Rau for useful discussions. The work was supported by the European Research Council through ERC-StG-TOPOLECTRICS-Thomale-336012. Y.I., T.M., and R.T. thank the DFG (Deutsche Forschungsgemeinschaft) for financial support through SFB 1170 (project B04). K.R. and R.V. thank the DFG for financial support through SFB/TR 49. J.R. is supported by the Freie Universität Berlin within the Excellence Initiative of the German Research Foundation. S.R. is supported by the DFG through SFB 1143. The work at the University of Waterloo was supported by the Canada Research Chair program (M.G., Tier 1) and by the Perimeter Institute (PI) for Theoretical Physics. Research at the Perimeter Institute is supported by the Government of Canada through Innovation, Science and Economic Development Canada and by the Province of Ontario through the Ministry of Research, Innovation and Science. We gratefully acknowledge the Gauss Centre for Supercomputing e.V. for funding this project by providing computing time on the GCS Supercomputer SuperMUC at Leibniz Supercomputing Centre (LRZ).

- [1] I. Pomeranchuk, *Zh. Eksp. Teor. Fiz.* **11**, 226 (1941).
- [2] P. Anderson, *Mater. Res. Bull.* **8**, 153 (1973).
- [3] P. Fazekas and P. W. Anderson, *Philos. Mag.* **30**, 423 (1974).
- [4] L. Balents, *Nature (London)* **464**, 199 (2010).
- [5] L. Savary and L. Balents, *Rep. Prog. Phys.* **80**, 016502 (2017).
- [6] Y. Zhou, K. Kanoda, and T.-K. Ng, *Rev. Mod. Phys.* **89**, 025003 (2017).
- [7] J. Villain, *Z. Phys. B* **33**, 31 (1979).
- [8] J. T. Chalker, P. C. W. Holdsworth, and E. F. Shender, *Phys. Rev. Lett.* **68**, 855 (1992).
- [9] R. Moessner and J. T. Chalker, *Phys. Rev. B* **58**, 12049 (1998).
- [10] A. B. Harris, A. J. Berlinsky, and C. Bruder, *J. Appl. Phys.* **69**, 5200 (1991).
- [11] B. Canals and C. Lacroix, *Phys. Rev. Lett.* **80**, 2933 (1998).
- [12] E. Berg, E. Altman, and A. Auerbach, *Phys. Rev. Lett.* **90**, 147204 (2003).
- [13] Y. Huang, K. Chen, Y. Deng, N. Prokof'ev, and B. Svistunov, *Phys. Rev. Lett.* **116**, 177203 (2016).
- [14] S. Yan, D. A. Huse, and S. R. White, *Science* **332**, 1173 (2011).
- [15] Y. Iqbal, F. Becca, S. Sorella, and D. Poilblanc, *Phys. Rev. B* **87**, 060405 (2013).
- [16] M. R. Norman, *Rev. Mod. Phys.* **88**, 041002 (2016).
- [17] Y.-C. He, M. P. Zaletel, M. Oshikawa, and F. Pollmann, *Phys. Rev. X* **7**, 031020 (2017).
- [18] H. J. Liao, Z. Y. Xie, J. Chen, Z. Y. Liu, H. D. Xie, R. Z. Huang, B. Normand, and T. Xiang, *Phys. Rev. Lett.* **118**, 137202 (2017).
- [19] G. Jackeli and G. Khaliullin, *Phys. Rev. Lett.* **102**, 017205 (2009).
- [20] J. Reuther, R. Thomale, and S. Trebst, *Phys. Rev. B* **84**, 100406 (2011).
- [21] S. M. Winter, Y. Li, H. O. Jeschke, and R. Valentí, *Phys. Rev. B* **93**, 214431 (2016).
- [22] M. Hermanns, I. Kimchi, and J. Knolle, *Ann. Rev. Condens. Matter Phys.* **9** (2018), doi: [10.1146/annurev-conmatphys-031117-053934](https://doi.org/10.1146/annurev-conmatphys-031117-053934).
- [23] S. Trebst, [arXiv:1701.07056](https://arxiv.org/abs/1701.07056).
- [24] S. M. Winter, A. A. Tsirlin, M. Daghofer, J. van den Brink, Y. Singh, P. Gegenwart, and R. Valentí, *J. Phys.: Condens. Matter* **29**, 493002 (2017).
- [25] H. R. Molavian, M. J. P. Gingras, and B. Canals, *Phys. Rev. Lett.* **98**, 157204 (2007).
- [26] S. Onoda and Y. Tanaka, *Phys. Rev. Lett.* **105**, 047201 (2010).
- [27] K. A. Ross, L. Savary, B. D. Gaulin, and L. Balents, *Phys. Rev. X* **1**, 021002 (2011).
- [28] M. J. P. Gingras and P. A. McClarty, *Rep. Prog. Phys.* **77**, 056501 (2014).
- [29] T.-H. Han, J. S. Helton, S. Chu, D. G. Nocera, J. A. Rodriguez-Rivera, C. Broholm, and Y. S. Lee, *Nature (London)* **492**, 406 (2012).
- [30] Z. Hao and O. Tchernyshyov, *Phys. Rev. B* **87**, 214404 (2013).
- [31] M. Punk, D. Chowdhury, and S. Sachdev, *Nat. Phys.* **10**, 289 (2014).
- [32] P. Mendels, F. Bert, M. A. de Vries, A. Olariu, A. Harrison, F. Duc, J. C. Trombe, J. S. Lord, A. Amato, and C. Baines, *Phys. Rev. Lett.* **98**, 077204 (2007).
- [33] A. Zorko, M. Herak, M. Gomilšek, J. van Tol, M. Velázquez, P. Khuntia, F. Bert, and P. Mendels, *Phys. Rev. Lett.* **118**, 017202 (2017).
- [34] B. Fák, E. Kermarrec, L. Messio, B. Bernu, C. Lhuillier, F. Bert, P. Mendels, B. Koteswararao, F. Bouquet, J. Ollivier, A. D. Hillier, A. Amato, R. H. Colman, and A. S. Wills, *Phys. Rev. Lett.* **109**, 037208 (2012).
- [35] E. Kermarrec, A. Zorko, F. Bert, R. H. Colman, B. Koteswararao, F. Bouquet, P. Bonville, A. Hillier, A. Amato, J. van Tol, A. Ozarowski, A. S. Wills, and P. Mendels, *Phys. Rev. B* **90**, 205103 (2014).
- [36] B. Bernu, C. Lhuillier, E. Kermarrec, F. Bert, P. Mendels, R. H. Colman, and A. S. Wills, *Phys. Rev. B* **87**, 155107 (2013).
- [37] H. O. Jeschke, F. Salvat-Pujol, and R. Valentí, *Phys. Rev. B* **88**, 075106 (2013).
- [38] Y. Iqbal, H. O. Jeschke, J. Reuther, R. Valentí, I. I. Mazin, M. Greiter, and R. Thomale, *Phys. Rev. B* **92**, 220404 (2015).
- [39] Z. Nussinov, C. D. Batista, B. Normand, and S. A. Trugman, *Phys. Rev. B* **75**, 094411 (2007).
- [40] A. Banerjee, S. V. Isakov, K. Damle, and Y. B. Kim, *Phys. Rev. Lett.* **100**, 047208 (2008).
- [41] N. Shannon, K. Penc, and Y. Motome, *Phys. Rev. B* **81**, 184409 (2010).
- [42] B. Normand and Z. Nussinov, *Phys. Rev. Lett.* **112**, 207202 (2014).
- [43] B. Normand and Z. Nussinov, *Phys. Rev. B* **93**, 115122 (2016).
- [44] Y. Okamoto, M. Nohara, H. Aruga-Katori, and H. Takagi, *Phys. Rev. Lett.* **99**, 137207 (2007).
- [45] A. C. Shockley, F. Bert, J.-C. Orain, Y. Okamoto, and P. Mendels, *Phys. Rev. Lett.* **115**, 047201 (2015).
- [46] M. Isobe and Y. Ueda, *J. Phys. Soc. Jpn.* **71**, 1848 (2002).
- [47] L. Clark, G. J. Nilsen, E. Kermarrec, G. Ehlers, K. S. Knight, A. Harrison, J. P. Attfield, and B. D. Gaulin, *Phys. Rev. Lett.* **113**, 117201 (2014).
- [48] D. Singh, G. Wilson-Short, D. Kasinathan, M. Suewattana, and M. Fornari, *Solid State Sci.* **9**, 604 (2007).
- [49] A. N. Yaresko, *Phys. Rev. B* **77**, 115106 (2008).
- [50] Y. V. Tymoshenko, Y. A. Onykiienko, T. Mueller, R. Thomale, S. Rachel, A. S. Cameron, P. Y. Portnichenko, D. V. Efremov, V. Tsurkan, D. L. Abernathy, J. Ollivier, A. Schneidewind, A. Piovano, V. Felea, A. Loidl, and D. S. Inosov, *Phys. Rev. X* **7**, 041049 (2017).
- [51] T. Nakamura and D. Hirashima, *J. Magn. Magn. Mater.* **310**, 1297 (2007).
- [52] D. Tsuneishi, M. Ioki, and H. Kawamura, *J. Phys.: Condens. Matter* **19**, 145273 (2007).
- [53] P. H. Conlon and J. T. Chalker, *Phys. Rev. B* **81**, 224413 (2010).
- [54] T. Okubo, T. H. Nguyen, and H. Kawamura, *Phys. Rev. B* **84**, 144432 (2011).
- [55] M. F. Lapa and C. L. Henley, [arXiv:1210.6810](https://arxiv.org/abs/1210.6810).
- [56] See Supplemental Material at <http://link.aps.org/supplemental/10.1103/PhysRevMaterials.1.071201> for details of density functional theory, pseudofermion functional renormalization group, and classical iterative energy optimization calculations.
- [57] H. Jeschke, I. Opahle, H. Kandpal, R. Valentí, H. Das, T. Sahad-Dasgupta, O. Janson, H. Rosner, A. Brühl, B. Wolf, M. Lang, J. Richter, S. Hu, X. Wang, R. Peters, T. Pruschke, and A. Honecker, *Phys. Rev. Lett.* **106**, 217201 (2011).
- [58] J. Reuther and P. Wölfle, *Phys. Rev. B* **81**, 144410 (2010).
- [59] J. Reuther and R. Thomale, *Phys. Rev. B* **83**, 024402 (2011).
- [60] J. Reuther, D. A. Abanin, and R. Thomale, *Phys. Rev. B* **84**, 014417 (2011).
- [61] W. Metzner, M. Salmhofer, C. Honerkamp, V. Meden, and K. Schönhammer, *Rev. Mod. Phys.* **84**, 299 (2012).

- [62] Y. Iqbal, R. Thomale, F. Parisen Toldin, S. Rachel, and J. Reuther, *Phys. Rev. B* **94**, 140408 (2016).
- [63] F. L. Buessen and S. Trebst, *Phys. Rev. B* **94**, 235138 (2016).
- [64] M. Hering and J. Reuther, *Phys. Rev. B* **95**, 054418 (2017).
- [65] M. L. Baez and J. Reuther, *Phys. Rev. B* **96**, 045144 (2017).
- [66] S. Depenbrock, I. P. McCulloch, and U. Schollwöck, *Phys. Rev. Lett.* **109**, 067201 (2012).
- [67] R. Suttor, C. Platt, J. Reuther, and R. Thomale, *Phys. Rev. B* **89**, 020408 (2014).
- [68] T. Yavors'kii, T. Fennell, M. J. P. Gingras, and S. T. Bramwell, *Phys. Rev. Lett.* **101**, 037204 (2008).
- [69] S. H. Lee, C. Broholm, W. Ratcliff, G. Gasparovic, Q. Huang, T. H. Kim, and S. W. Cheong, *Nature (London)* **418**, 856 (2002).
- [70] S. Okumura, H. Kawamura, T. Okubo, and Y. Motome, *J. Phys. Soc. Jpn.* **79**, 114705 (2010).
- [71] The value of \mathbf{k}_{QSL} changes only minimally with temperature. The RG flows tracked at these different \mathbf{k}_{QSL} vectors all show paramagnetic behavior.
- [72] Z. Nussinov, [arXiv:cond-mat/0105253](https://arxiv.org/abs/cond-mat/0105253).
- [73] I. Kimchi and A. Vishwanath, *Phys. Rev. B* **89**, 014414 (2014).
- [74] G.-W. Chern, R. Moessner, and O. Tchernyshyov, *Phys. Rev. B* **78**, 144418 (2008).
- [75] Y. Iqbal, W.-J. Hu, R. Thomale, D. Poilblanc, and F. Becca, *Phys. Rev. B* **93**, 144411 (2016).
- [76] Y. Iqbal, P. Ghosh, R. Narayanan, B. Kumar, J. Reuther, and R. Thomale, *Phys. Rev. B* **94**, 224403 (2016).
- [77] L. Messio, C. Lhuillier, and G. Misguich, *Phys. Rev. B* **83**, 184401 (2011).
- [78] J. H. Kim and J. H. Han, *Phys. Rev. B* **78**, 180410 (2008).
- [79] F. J. Burnell, S. Chakravarty, and S. L. Sondhi, *Phys. Rev. B* **79**, 144432 (2009).
- [80] C. Hickey, L. Cincio, Z. Papić, and A. Paramekanti, *Phys. Rev. B* **96**, 115115 (2017).
- [81] Y. Machida, S. Nakatsuji, S. Onoda, T. Tayama, and T. Sakakibara, *Nature (London)* **463**, 210 (2010).
- [82] S. B. Lee, A. Paramekanti, and Y. B. Kim, *Phys. Rev. Lett.* **111**, 196601 (2013).
- [83] S. Bieri, L. Messio, B. Bernu, and C. Lhuillier, *Phys. Rev. B* **92**, 060407 (2015).
- [84] S. Bieri, C. Lhuillier, and L. Messio, *Phys. Rev. B* **93**, 094437 (2016).
- [85] I. Dzyaloshinsky, *J. Phys. Chem. Solids* **4**, 241 (1958).
- [86] T. Moriya, *Phys. Rev.* **120**, 91 (1960).
- [87] M. Elhajal, B. Canals, R. Sunyer, and C. Lacroix, *Phys. Rev. B* **71**, 094420 (2005).
- [88] V. N. Kotov, M. Elhajal, M. E. Zhitomirsky, and F. Mila, *Phys. Rev. B* **72**, 014421 (2005).
- [89] K. Riedl, D. Guterding, H. O. Jeschke, M. J. P. Gingras, and R. Valentí, *Phys. Rev. B* **94**, 014410 (2016).